

RESEARCH PAPER

## Experimental Investigation and Prediction of Pour Point Using Artificial Intelligence

Maryam Mahmoudi Kouhi<sup>1</sup>, Elnaz Khodapanah<sup>2\*</sup>

1. MSc Petroleum Engineering, Faculty of Petroleum and Natural Gas Engineering, Sahand University of Technology

2. Associate Professor of Petroleum Engineering, Faculty of Petroleum and Natural Gas Engineering, Sahand University of Technology, Sahand New Town, Tabriz, Iran, P.O.Box: 5331817634

### ARTICLE INFO

Article History:

Received 17 January 2021

Revised 12 September 2021

Accepted 13 September 2021

Keywords:

Pour point

Multilayer perceptron neural network

Radial basis neural network

Wax content

Cloud point

### ABSTRACT

Pour point as an important physical property of crude oil is a measure of its low temperature fluidity. The accurate determination of this property is of significance as the temperature decrease below the pour point of the crude oil causes severe production and transportation problems. In this study, for the first time, two types of artificial neural networks (ANNs), including multilayer perceptron (MLP) and radial basis function (RBF), were proposed to predict the pour point. First, the MLP network was modeled and evaluated using different methods. To this end, the optimal number of the input parameters and the best activation function were examined. The results showed that the best predictive MLP network model is constructed using two parameters of wax content and cloud point and SoftMax-SoftMax activation function. The regression of training, validation, and testing datasets of the constructed MLP were 79.5%, 74.1%, and 76.8%, respectively. To validate the constructed MLP-ANN, some experiments were conducted on an oil sample. The dataset obtained from the experiments was then used to predict the pour point. The absolute error of 0.94 °C indicated the great performance of the MLP-ANN in predicting the pour point. Finally, the prediction performance of the MLP-ANN was compared to the RBF-ANN. The results showed the higher predictive accuracy of the MLP-ANN in comparison with the RBF-ANN. Based on the obtained results, the proposed MLP-ANN can be used with confidence in lieu of the expensive and time-consuming laboratory measurements to determine the pour point of crude oils.

### How to cite this article

Mahmoudi Kouhi M, Khodapanah E. Experimental Investigation and Prediction of Pour Point Using Artificial Intelligence, Journal of Oil, Gas and Petrochemical Technology, 2022; 9(1): 49-74. DOI:10.22034/jogpt.2023.268812.1085.

### 1. INTRODUCTION

Crude oil is a mixture that mainly contains hydrocarbons, sulfur, nitrogen, and metals[1]. Paraffin wax is a mixture of alkanes composed of linear and branched chains in the range of twenty

to forty carbon atoms, which precipitates under suitable conditions. It may be present in solid or liquid states, depending on temperature and pressure [2-4].

Pour point is an important oil property, defined as the lowest temperature below which oil does not flow under the influence of gravity. It is

\* Corresponding Author Email: [khodapanah@sut.ac.ir](mailto:khodapanah@sut.ac.ir)

measured according to ASTM D97. In this method, the sample is heated to a certain temperature to ensure that the wax crystals are dissolved in the oil. After that, the sample is cooled. During the cooling process, it is placed horizontally for each three degrees decrease in temperature to observe whether the fluid is movable in five seconds. The temperature at which the fluid movement is not observed is added to 3 °C and reported as the pour point temperature [5-7].

Wax has a complex structure and its deposition imposes a very costly problem on the oil industry. Therefore, it has been widely studied by researchers over the past decades. For instance, in submarine pipelines, solving the problem of wax deposition is of particular importance, because oil production in colder regions encounters severe wax deposition problems. Wax deposition in pipelines at temperatures below the cloud point causes the gelation of the fluid, which results in a non-Newtonian fluid behavior and an increase in its effective viscosity as the temperature of the waxy crude oil reaches the pour point [8].

In recent years, soft computing techniques, due to their high accuracy and low costs, have received considerable attention in different fields, including oil and gas industry [9].

Artificial neural networks (ANNs), which are considered as a branch of artificial intelligence, have the ability to learn, store, and retrieve information if an appropriate database is provided. An artificial neural network consists of a number of connected nodes and computational models. Complex relationships can be modeled using the artificial neural networks. The ability to process a large database and generalize the relationships between different variables is a key feature of the neural networks. The research and development process in the oil and gas industry is moving towards the use of artificial intelligence (AI) algorithms and changing machine learning concepts [10, 11].

An artificial neural network is a software implementation that acts like a biological element of the central nervous system of the human brain, but the real picture of the human neural network system is not just a simplification, abstraction, and simulation. Natural neurons receive signals through synapses on dendrites or neurons' membranes. When the received signals are strong enough (more than a certain threshold), the neuron is activated and emits the

signal by the axon. This sign might ship off another neurotransmitter and may actuate different neurons. In recent years, the use of artificial neural network modeling techniques has resulted in their ability to accurately predict small data sets instead of large data sets that require costly and time-consuming studies and experiments. By using these techniques, neuroscience, mathematical and computational analysis, learning systems, engineering design and application, and chemical and environmental engineering, have been successful. The artificial neural networks as shown in Figure 1, have a scientific basis, which begins with a biological neuron [12, 13].

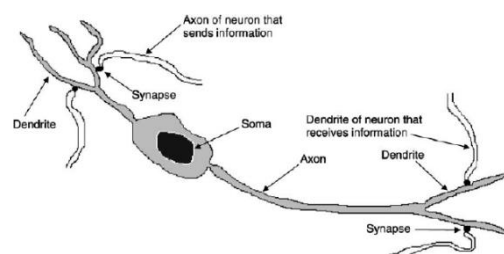


Figure 1. Biological neurons of the human brain [14]

### Multilayer perceptron (MLP) neural network

The MLP neural network is one of the well-known types of ANNs, which has a high ability to detect nonlinear relationships that rely on a set of inputs for specific purposes. MLP belongs to the supervised learning category. An MLP-ANN, as shown in Figure 2, consists of three layers: input layer, hidden layer, and output layer [15].

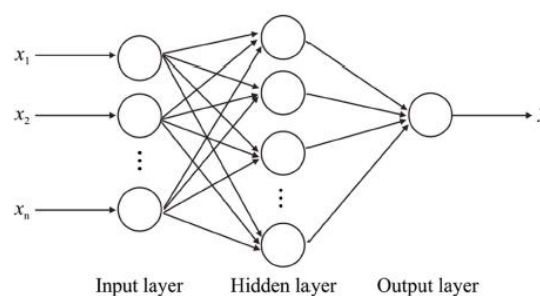


Figure 2. Structure of a multilayer perceptron neural network [16]

These networks are essentially a combination of neurons, biases assigned to neurons, connections between them, and weights assigned to these connections. The learning process is based on the

input and target data sets and training algorithms. Mathematically, a neuron can be defined by the following two equations:

$$y_k = f(u_k + b_k) \quad (1)$$

$$u_k = \sum_{i=1}^N w_{ki}x_i \quad (2)$$

$x_1, x_2, \dots, x_n$  represent the input signals,  $w_{k1}, w_{k2}, \dots, w_{kn}$  are the weights of the neuron connections,  $u_k$  is the linear hybrid output between the weighted inputs,  $b_k$ ,  $f$  is the activation function, and  $y_k$  is the output signal of the neurons.

The MLP-ANN can be trained using the back propagation (BP) algorithm, which is a learning method based on the error correction law. The network generates the outputs by processing the received input data. Comparing the target values and the network output, the error value is calculated. The weights and biases are then adjusted to minimize the errors. The training process continues until the network reaches a predefined acceptable minimum. The error function used for this purpose is usually the mean squared error (MSE) [17].

### Radial basis function (RBF) neural network

One of the basic features of the RBF neural network is learning. First, a set of training samples is provided with the ideal input and output data, and then the network is trained by these samples. The training ends when the actual network input corresponds to the ideal output. Otherwise, the weights are modified so that the desired result is achieved. Figure 3 shows the structure of an RBF neural network system, which is a specific classification of a data prediction neural network with an input layer, a hidden layer, and a linear output layer. Inputs come from some sources. The second layer is a hidden layer of the nonlinear processing units called RBF. The output layer reacts to the activation patterns applied to the input layer. The network can be intended to perform a nonlinear mapping from the input layer to the hidden space, and linear mapping from the hidden space to the output layer. This is a point of view in neural network research that is widely used in many situations such as nonlinear control, image processing, and series analysis. Compared to other types of artificial neural networks, the

RBF neural network has a simpler structure, faster learning, and good approximate properties [18].

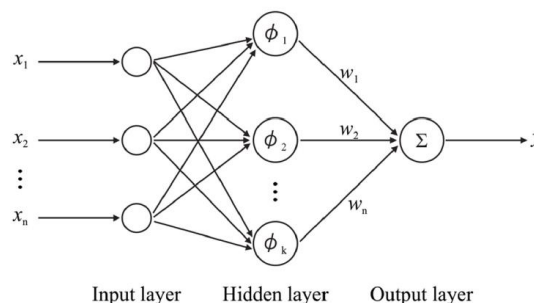


Figure 3. Structure of radial basis function [18]

In 2012, Arpit et al. examined the correlation based on linear and artificial neural networks to determine the pour point and cloud point of medium and heavy distillations. The parameters studied in this work were density and distillation temperature. Linear correlation is simple and easy, but the errors associated with this correlation are higher than ANN. The best neural network correlation was obtained with seven neurons for the pour point and 25 neurons for the cloud point. The linear correlation showed the dependence of the pour point and the cloud point with each of the selected properties. Also, a correlation was observed for both pour point and cloud point in the form of neural network with average absolute errors of 3.8 and 3.6 °C, respectively [19].

In 2017, Hu et al. modeled the pour point of crude oil based on Bayesian regularized artificial neural network (BRANN). The results showed that this model not only has a good ability to adapt to educational data, it also has a good ability to predict test data [20].

The purpose of this study is to accurately predict the pour point of different types of crude oils with different characteristics based on the artificial neural networks. For the first time, two types of artificial neural networks, including MLP and RBF were proposed and evaluated in terms of their capability in predicting the pour point. To this end, several parameters including API, wax content, cloud point, and saturate, aromatic, resin, and asphaltene (SARA) fractions were examined as inputs to the MLP neural network. The most effective parameters in predicting the pour point were determined. Furthermore, the Tansig, Logsig, and Softmax activation functions were tested to select the best function based on the predictive

accuracy of the MLP-ANN. Next, the constructed network was validated using the data set of an oil sample obtained in the laboratory. Finally, the proposed MLP-ANN was compared to the RBF-ANN in terms of their accuracy in predicting the pour point.

## 2. Research Method

In this paper, two types of artificial neural networks including MLP and RBF were constructed to predict the pour point of crude oils. To this end, 114 datasets including 912 experimental data were gathered from open literature [21-41] and used to train and test the proposed networks. The datasets are given in Appendix A. Each dataset contains eight experimental data of API, wax content, cloud point, and saturate, aromatic, resin, and asphaltene (SARA) fractions, and pour point. The datasets cover a wide range of pour point from -42 to 42 °C, and different types of crude oils including light, medium and heavy oils according to the values of API.

Furthermore, some experiments including API measurement, wax content determination, SARA (saturate, aromatic, resin and asphaltene) analysis, cloud point, and pour point measurements were conducted on an oil sample to validate the modeled neural networks.

To construct the efficient neural network, first, different networks were modeled using

each of the seven parameters including API, wax content, cloud point, and SARA fractions as input. Second, based on the obtained results of the first step, the most efficient parameters were used simultaneously as inputs to the neural network. Next, all the seven parameters were simultaneously used as inputs to examine and compare the performance of the modeled ANNs in predicting the pour point. Selecting the most predictive neural network, different activation functions were investigated in terms of their performance in the prediction of the pour point. Finally, the constructed MLP and RBF neural networks were compared with each other.

Table 1 shows the experimental properties obtained for an oil sample and used to validate the constructed neural networks.

The experimental methods used to measure the above-mentioned oil properties are as the following:

Pour point: This property was measured based on ASTM D97.

Cloud point: The temperature corresponding to the first formation of wax crystals was measured using the viscometer method. To this end, a 300 SVM viscometer was employed and the viscosity of the oil sample was measured at different temperatures. The results are shown in Figure 4.

**Table 1.** Experimental data of an oil sample used to validate the neural networks

Pour point (°C)	Cloud point (°C)	°API	Wax content (wt%)	Saturate (wt%)	Aromatic (wt%)	Resin (wt%)	Asphaltene (wt%)
0	32	11.9	29.4	28.5	35.2	19.6	16.7

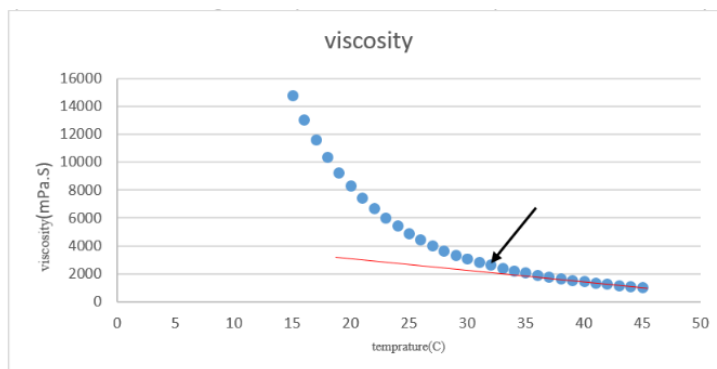


**Figure 4.** Viscosity of the oil sample given in Table 1 measured at different temperatures

The temperature of the point corresponding to the change in the slope of the curve is reported as the cloud point temperature.

**Wax content:** The modified UOP 46-64 method was used to measure the wax content of the crude oil.

**Asphaltene content:** This test was conducted according to ASTM D6560.

**SARA analysis:** After determining the asphaltene content of the crude oil, the residual oil from which the asphaltene was extracted was used to measure the saturate, aromatic, and resin contents. This test was performed using a two-column glass apparatus shown in Figure 5. The lower column contains silica gel and alumina and the upper column contains alumina.



Figure 5. SARA Analysis Apparatus

### 3. Results and Discussion

In this section, the modeled neural networks, their validation, and comparison of the constructed networks in predicting the pour point are discussed.

#### 3.1. MLP-ANN

The network structure has the desired number of inputs, two hidden layers that have five and three neurons, respectively, and an output layer. The number of neurons in the hidden layers is estimated by trial and error method. To this end, different combinations of the number of neurons in the hidden layers are selected and the neural network is implemented for each combination. The best combination is selected based on the regression values of the neural network. According to this procedure, the number of neurons was obtained as three and five in the first and second hidden layers, respectively.

In order to transform the activation level of a neuron into an output signal based on the given set of inputs, the activation function is used in neural networks. Different types of the activation functions are shown in Table 2. The subsequent neural network models were executed based on two hidden layers with the combination of the activation functions given in Table 2.

Table 2. Activation functions used in neural networks

Run number	1	2	3	4	5	6	7	8	9
Activation function	Tansig-Tansig	Logsig-Logsig	Softmax-Softmax	Tansig-Logsig	Logsig-Tansig	Softmax-Tansig	Softmax-Logsig	Tansig-Softmax	Logsig-Softmax

#### Effect of API on pour point prediction:

Considering the API data as input and the pour point data as output of the MLP-ANN, a model was implemented, the results of which are shown in Figure 6. 70% of the data was allocated to training, 15% to validation and 15% to testing. The regression values of the training, validation and testing represent the performance of the prediction based on the training, validation and testing sets, respectively. The mean squared error (MSE), defined by the following equation, indicates the average of the squares of the difference between the network output and the

target output. MSE is defined as the following:

Where  $(OUT)_i$ ,  $(NET)_i$  and  $N$  denote the observed value, predicted value, and the number of data points, respectively.

$$MSE = \frac{\sum_{i=1}^N [(OUT)_i - (NET)_i]^2}{N} \quad (3)$$

The mean squared error (MSE) in predicting the pour point using API as the network input parameter is shown in Figure 7. The low regression values of training, validation, and testing sets indicate that the modeled neural network using API data as

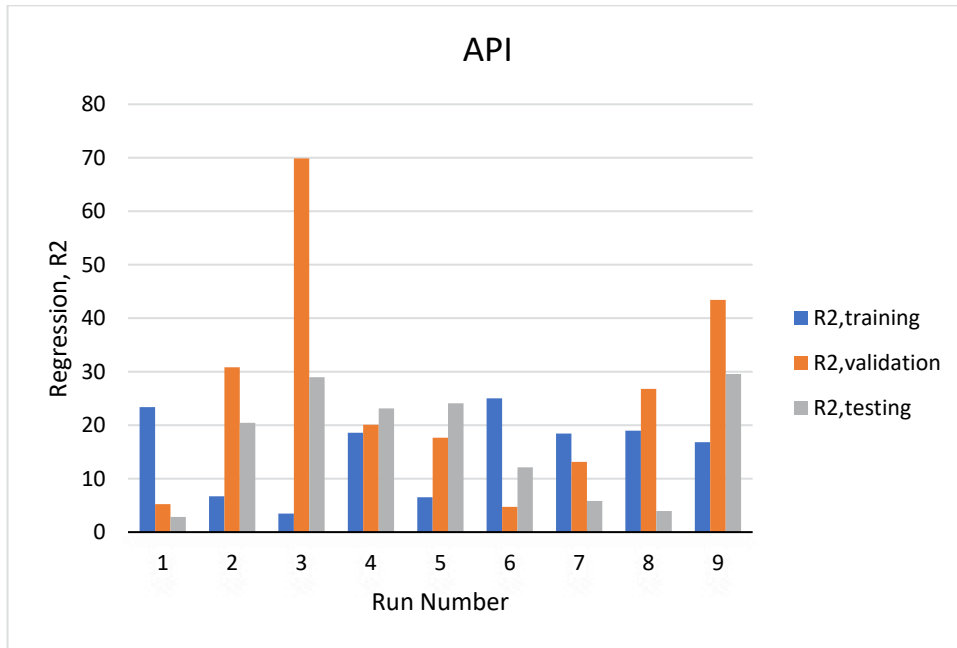


Figure 6. Regression of training, validation and testing datasets of the ANN using API as the input parameter

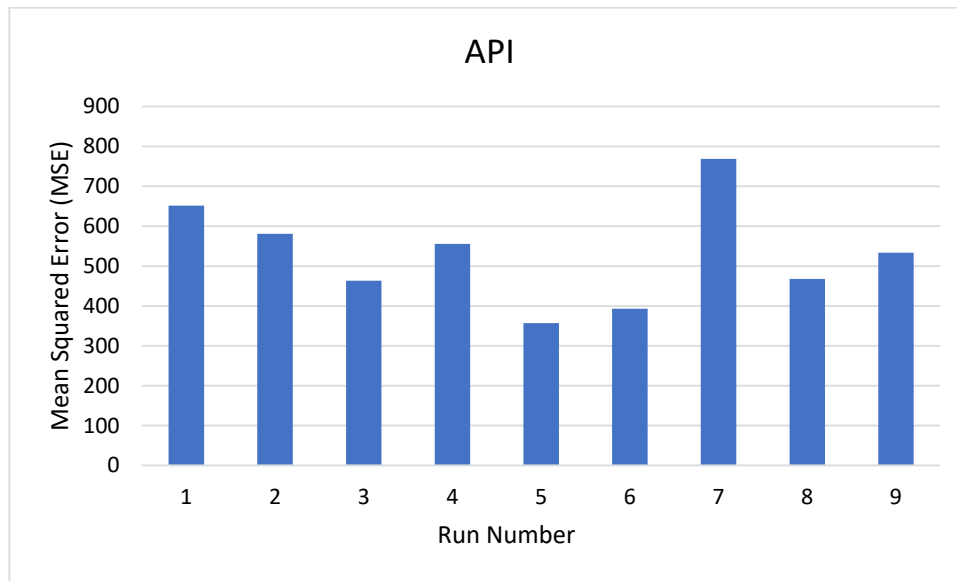


Figure 7. MSE of the ANN using API as the input parameter

inputs cannot provide satisfactory predictions of the pour point (Figure 6). The regression value of the overall set is obtained as 30%, confirming the poor performance of this network in predicting the pour point. Consequently, using only API as input to the neural network is not effective for the prediction purpose.

**Effect of wax content on pour point prediction:** To investigate the effect of wax content on the pour point, this property was considered as input to the neural network. Figure 8 and Figure 9 show the regression values and MSE of the modeled ANN, respectively.

According to Figure 8, the regression value of

the overall set is 55%, which is much higher than that obtained using API as the input parameter. This indicates that wax content is more effective than API in predicting the pour point. Therefore, wax content can be used as one of the significant input parameters of the neural network.

**Effect of SARA fractions on pour point prediction:**

Each of the saturate, aromatic, resin and asphaltene fractions was implemented separately as the input to the ANN. Figures 10 shows the effect of the saturate content on the pour point prediction in terms of the regression values of the ANN. The corresponding values of MSE are shown in Figure 11.

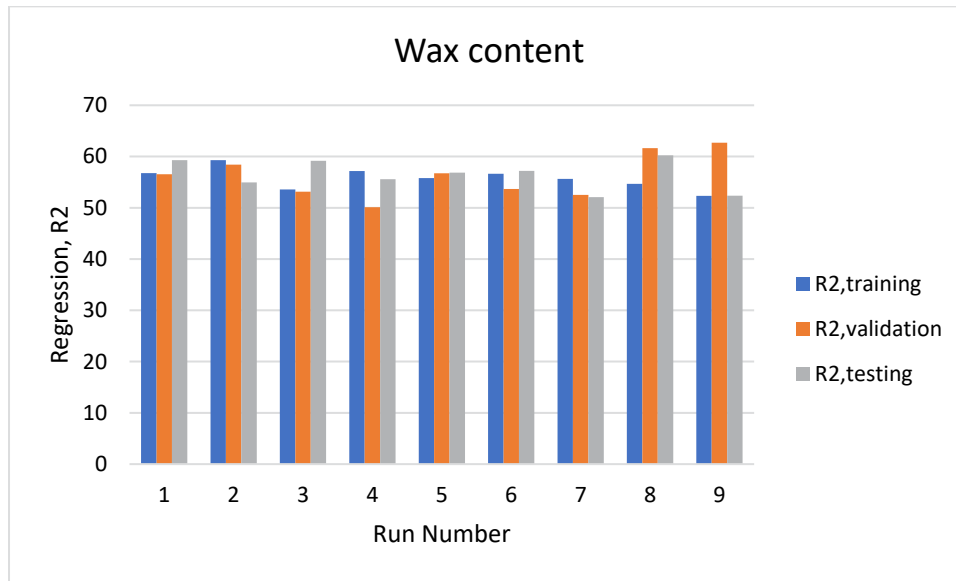


**Figure 8.** Regression of training, validation and testing datasets of the ANN using wax content as the input parameter

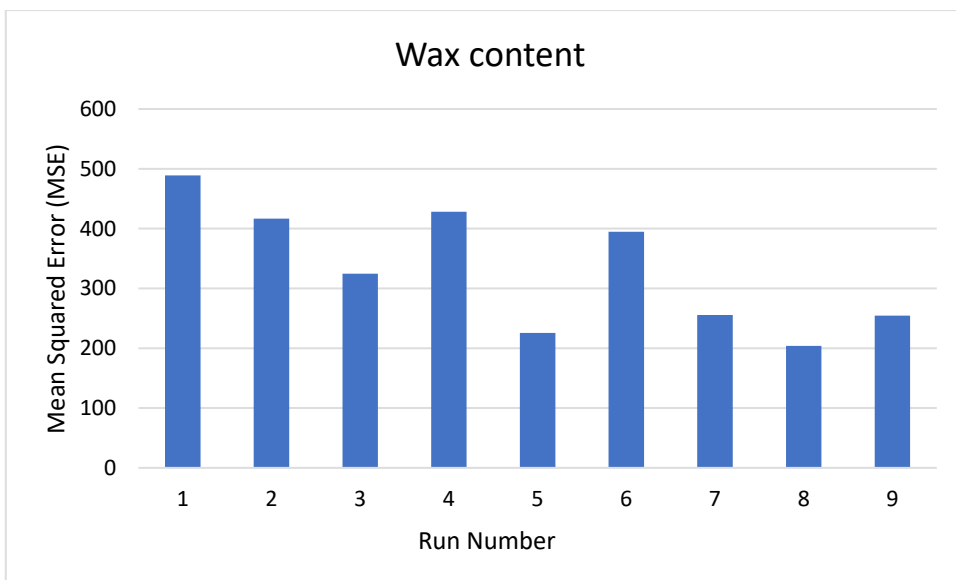


**Figure 9.** MSE of the ANN using wax content as the input parameter

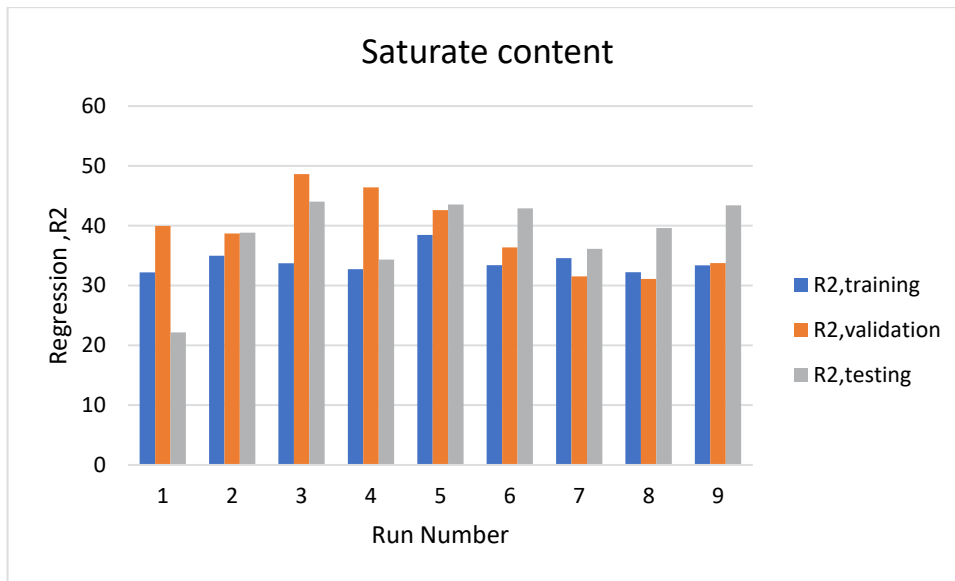


Figure 10. Regression of training, validation and testing datasets of the ANN using saturate content as the input parameter

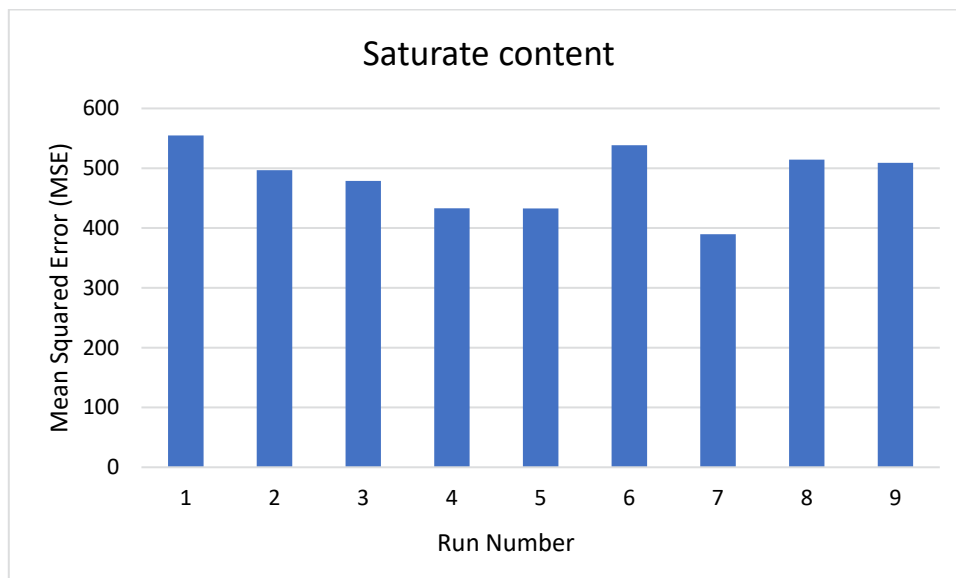


Figure 11. MSE of the ANN using saturate content as the input parameter

As Figure 10 and Figure 11 show, when using saturate fraction as the input parameter, the predictive accuracy of the ANN is higher than that obtained by means of API. However, the modeled ANN has lower prediction performance than the ANN constructed using the wax content as the input parameter because the regression value of the overall set in the former case is 38.3% (Figure

10). Additionally, MSE values do not yield in satisfactory results for the pour point prediction (Figure 11).

Figure 12 and Figure 13 show the accuracy evaluation of the modeled ANN using the aromatic fraction of crude oil as the input parameter. According to these figures, aromatic content does not significantly affect the pour point and

cannot be a potential parameter in assessing this property. As it can be seen from Figure 12, the regression value of the overall set is about 38.7%. Consequently, similar to the saturate fraction, the aromatic fraction does not have a significant effect on the prediction of pour point.

The regression and MSE of the modeled ANN using resin content as the input parameter are shown in Figure 14 and Figure 15, respectively. In this case, the regression value of the overall set is less than 30%, which represents the low significance of the resin fraction in the pour point prediction (Figure 14).

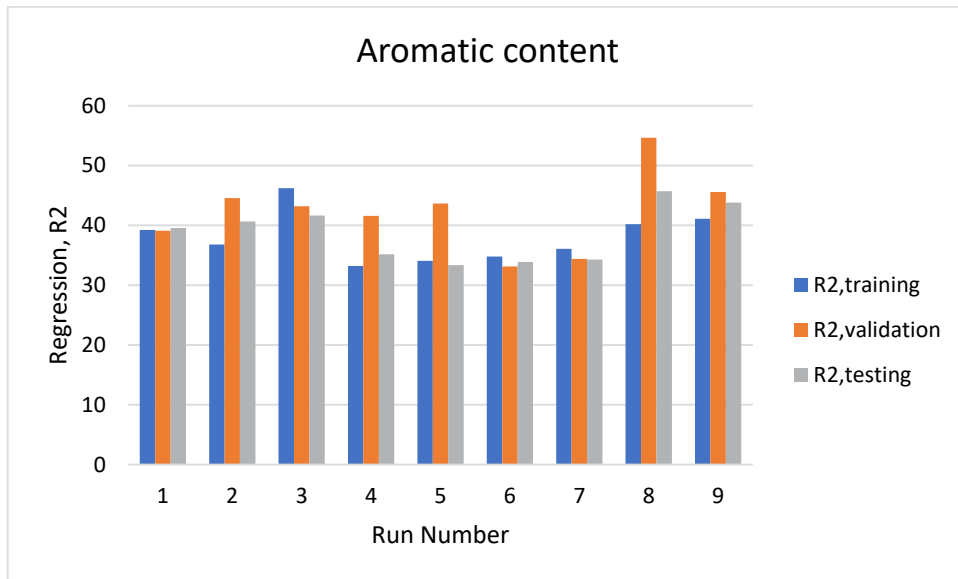


Figure 12. Regression of training, validation and testing datasets of the ANN using aromatic content as the input parameter

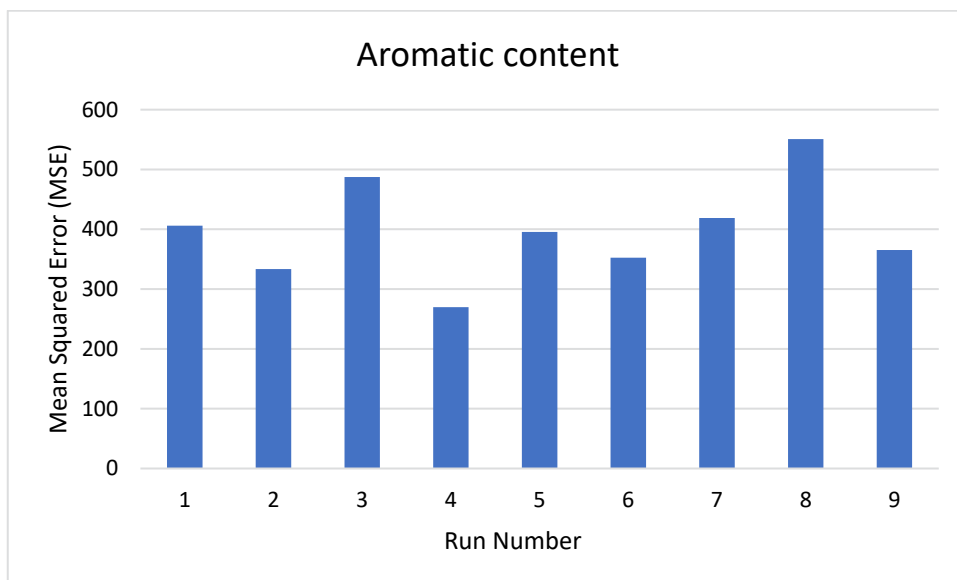


Figure 13. MSE of the ANN using aromatic content as the input parameter

The large values of the MSE also confirm the poor predictive accuracy of the ANN.

The last parameter of the SARA analysis used as input to the neural network is the asphaltene content of crude oil. To investigate the impact of this parameter on pour point, Figure 16 and Figure

17, representing, respectively, the regression and MSE of the corresponding ANN are depicted. As it can be seen from Figure 16, the asphaltene fraction has a very low impact on the results of pour point prediction.

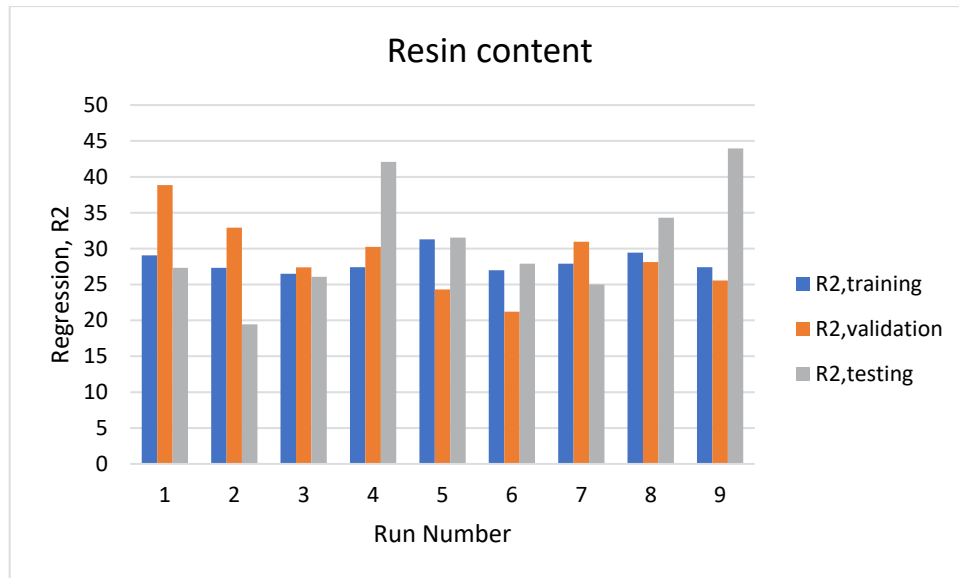


Figure 14. Regression of training, validation and testing datasets of the ANN using resin content as the input parameter

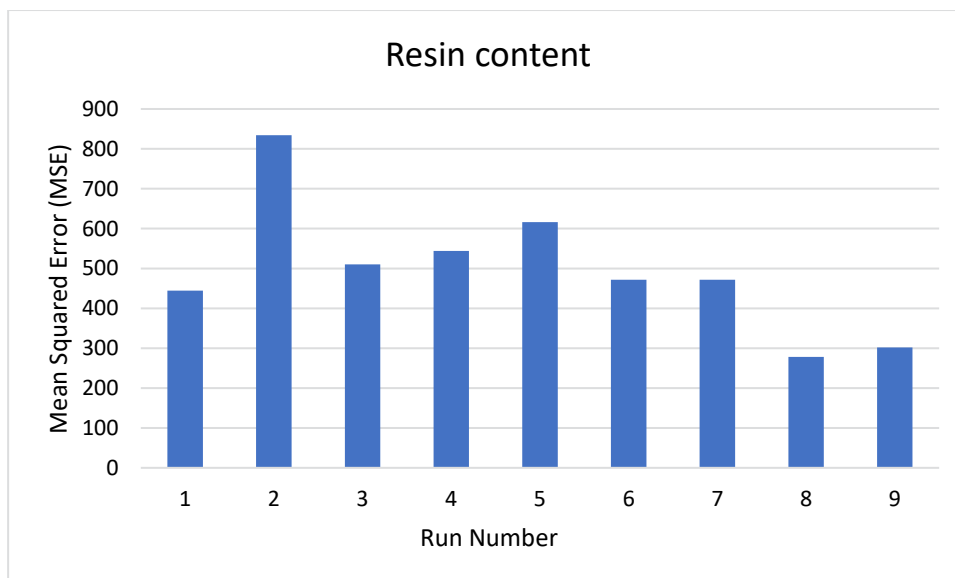


Figure 15. MSE of the ANN using resin content as the input parameter

In this case, the regression value of the overall set is 22.7%. This may be due to the conflicting effect of asphaltene fraction on the pour point of waxy oils. Depending on

its amount, asphaltene can have positive or negative effects on the pour point. Therefore, this parameter is not suitable to be used as the input to the neural network.

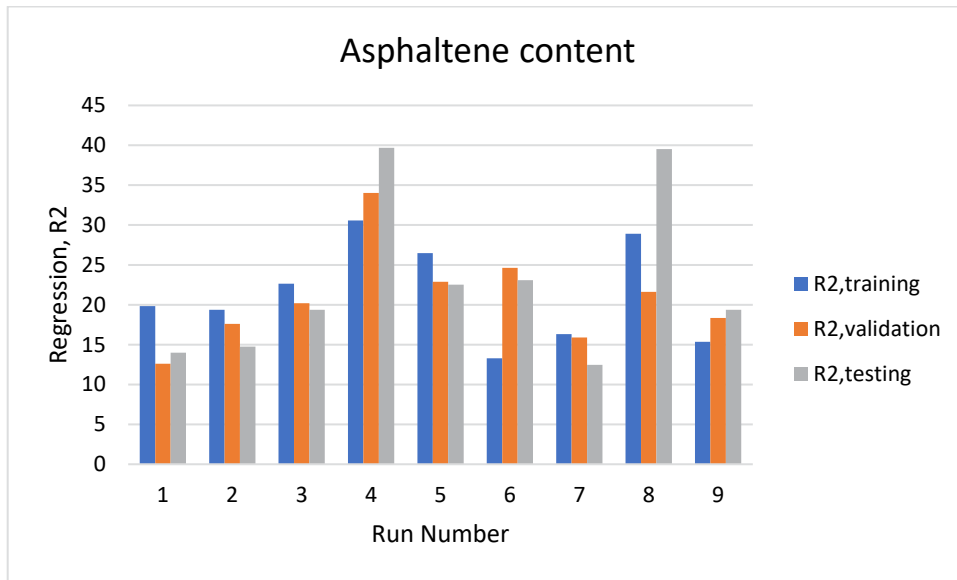


Figure 16. Regression of training, validation and testing datasets of the ANN using asphaltene content as the input parameter

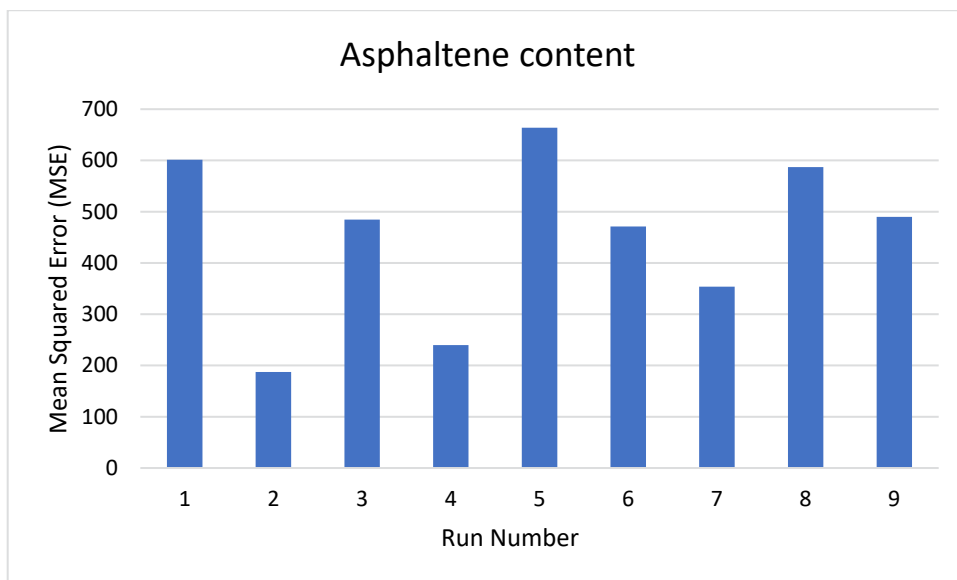


Figure 17. MSE of the ANN using asphaltene content as the input parameter

**Effect of cloud point on pour point prediction:**

In this case, the cloud point temperature was considered as the input parameter to predict the pour point. The regression of this prediction is shown in Figure 18. According to Figure 18,

the regression value of the overall set is 66.1%. It is observed from the figure that cloud point is the most effective parameter among the seven parameters in the datasets used as inputs to the neural network.

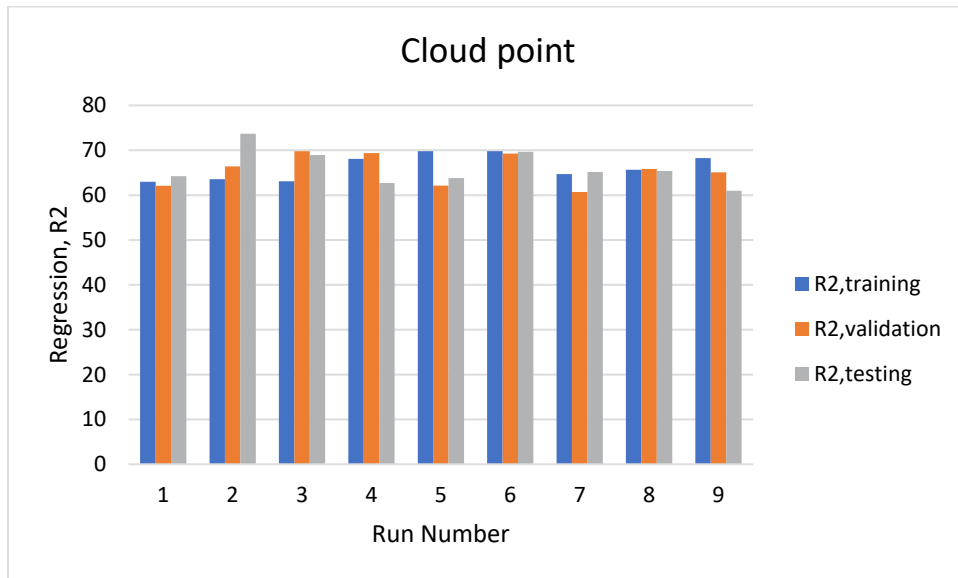


Figure 18. Regression of training, validation and testing datasets of the ANN using cloud point as the input parameter

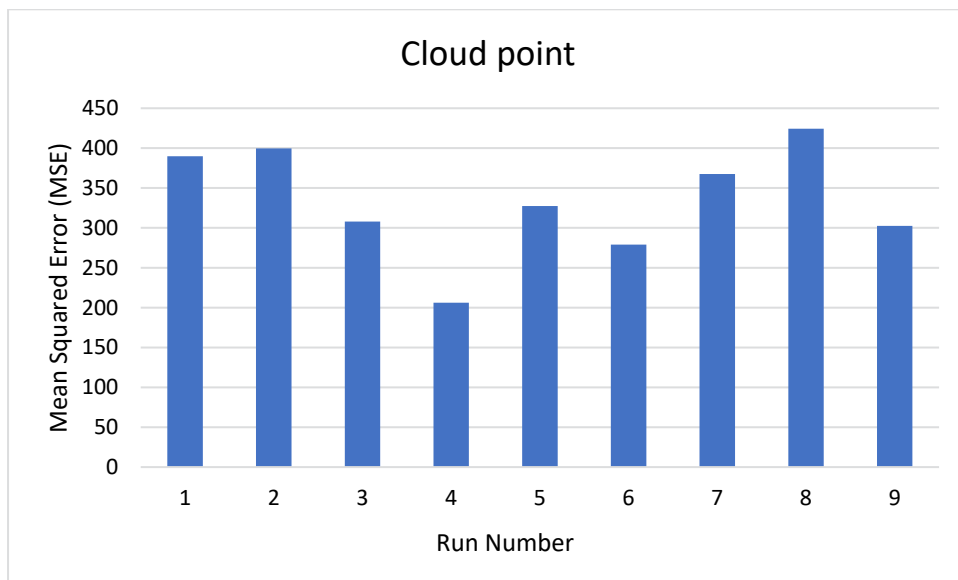


Figure 19. MSE of the ANN using cloud point content as the input parameter

The highest performance prediction of the mentioned ANN is also confirmed according to the lowest MSE shown in Figure 19. The high significance of this parameter on the pour point prediction can be attributed to the

interdependency of the cloud point and the pour point. The cloud point is the temperature at which the first crystal of wax is formed. As mentioned earlier, the temperature below which the crude oil does not flow is the pour point.

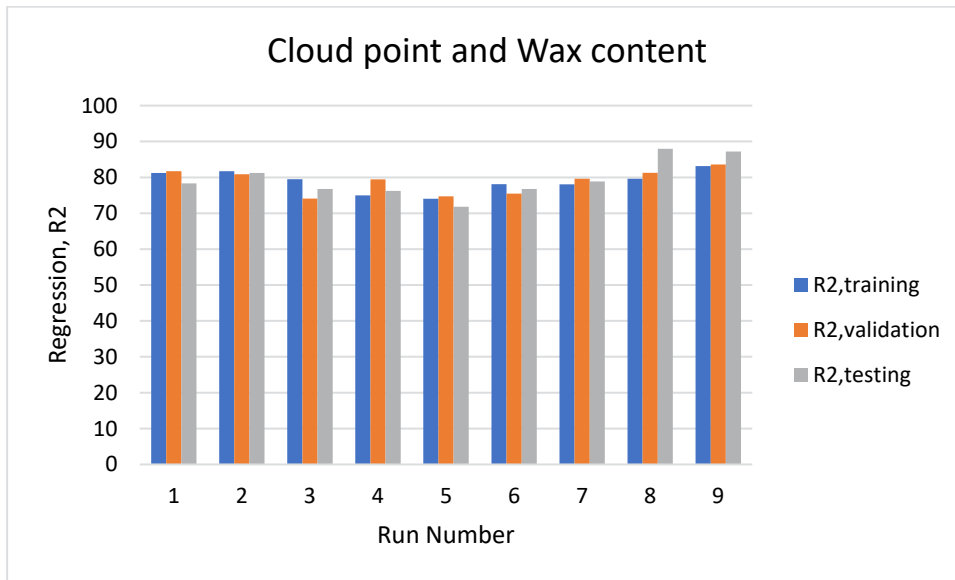


Figure 20. Regression of training, validation and testing datasets of the ANN using cloud point and wax content as the input parameters

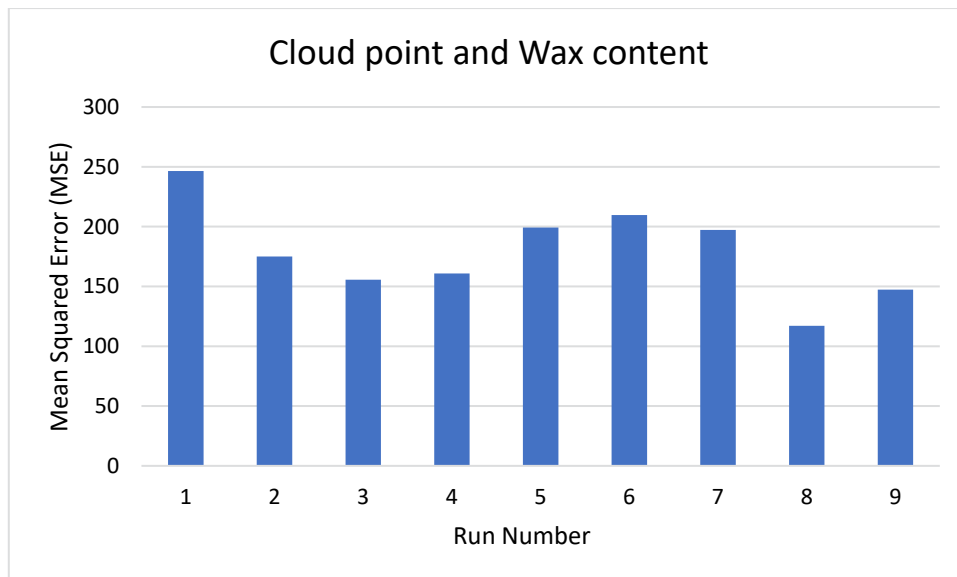
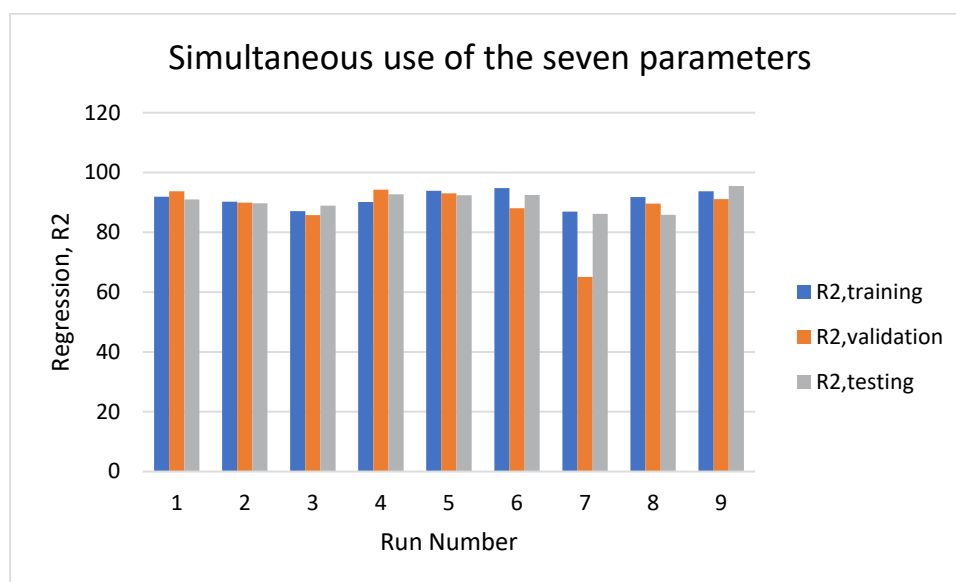


Figure 21. MSE of the ANN by simultaneous use of cloud point and wax content as the input parameters

**Simultaneous effect of wax content and cloud point on pour point prediction:** Based on the individual effects of the above-mentioned seven parameters, it was found that the two parameters of wax content and cloud point exhibit the highest impact on the pour point prediction. For this reason, the simultaneous effect of these two parameters on the pour point was investigated. Figure 20 and Figure 21 show, respectively, the regression and MSE of the modeled ANN by the simultaneous use of wax content and cloud point as the input parameters. As it can be seen from Figure 20, when these two parameters are implemented simultaneously, the regression of the testing set is 79.5%. Therefore, the corresponding ANN indicates superior accuracy in predicting the

pour point with respect to the previous models. According to the MSE shown in Figure 21, the same conclusion can be drawn.

In order to examine the performance of the ANNs in relation to the activation functions, different combinations of the functions shown in Table 2 were implemented. All the mentioned neural network models were executed using these combinations, the results of which are depicted in the corresponding regression and MSE figures. As the regression and MSE figures show, the Softmax-Softmax function leads to the neural network with the highest performance accuracy. The low accuracy of the ANNs implementing other activation functions may be due to the overfitting of these types of networks.



**Figure 22.** Regression of training, validation and testing datasets of the ANN by simultaneous use of the seven parameters

In all the mentioned neural networks, the pureline function was implemented in the output layer. The Softmax-Softmax activation function improves the performance of the pureline function by normalizing the data in the hidden layers. This function also eliminates the noises in the hidden layers.

**Effect of simultaneous use of all the examined parameters on pour point prediction:** In this case, all the seven mentioned parameters are implemented simultaneously as the input to the neural network. The regression values of the

training, validation and testing sets using this neural network are depicted in Figure 22.

Based on the results obtained from the implemented models, the most efficient neural network is obtained when using the two parameters of cloud point and wax content as the input. This modeled network is selected as the optimum one because of its higher regression values than the other constructed networks. The comparison of this model with the model constructed by means of the seven input parameters of API, wax content, cloud point, and SARA fractions reveals that using

the two parameters leads to the network with the comparable predictive accuracy to that modeled using the seven parameters. This becomes more important when considering the expensive and time-consuming SARA analysis to collect the related data as the input to the neural network.

### 3.2. RBF-ANN

The RBF neural network was also constructed to predict the pour point. For this purpose, the best case of the examined MLP-ANNs in terms of the input parameters was implemented. Therefore, the RBF-ANNs were constructed using the two parameters of wax content and cloud point as input.

Table 3 shows the accuracy of the RBF in relation with the number of neurons. As it can be seen from the table, the better prediction is obtained by implementing ten neurons.

**Table 3.** Accuracy of the RBF-ANN in terms of the number of neurons

Run number	Number of neurons	R2, testing dataset (%)	R2, overall dataset (%)	MSE
1	5	56.9	86.4	118.8
2	10	51.5	91.3	95.1

**Table 4.** Input parameters of the modeled neural networks

Neural network model	Input parameters	Activation function
1	Wax content, Cloud point	Tansig-Tansig
2	Wax content, Cloud point	Logsig-Logsig
3	Wax content, Cloud point	Softmax-Softmax
4	Wax content, Cloud point	Tansig-Logsig
5	Wax content, Cloud point	Logsig-Tansig
6	Wax content, Cloud point	Softmax-Tansig
7	Wax content, Cloud point	Softmax-Logsig
8	Wax content, Cloud point	Tansig-Softmax
9	Wax content, Cloud point	Logsig-Softmax

### 3.3. Validation of the models

To validate the modeled neural networks, the laboratory data set of the oil sample shown in Table 1 was used.

Figure 23 shows the results of pour point prediction using the modeled MLP neural networks (Table 4) for the experimental dataset given in Table 1. As it can be observed from the figure, the best prediction of the pour point is obtained when using the two parameters of cloud point and wax content as input to the MLP-ANN and implementing the Softmax-Softmax activation function in the hidden layers. According to Table 1, the experimental value of the pour point for this oil sample is 0 °C.

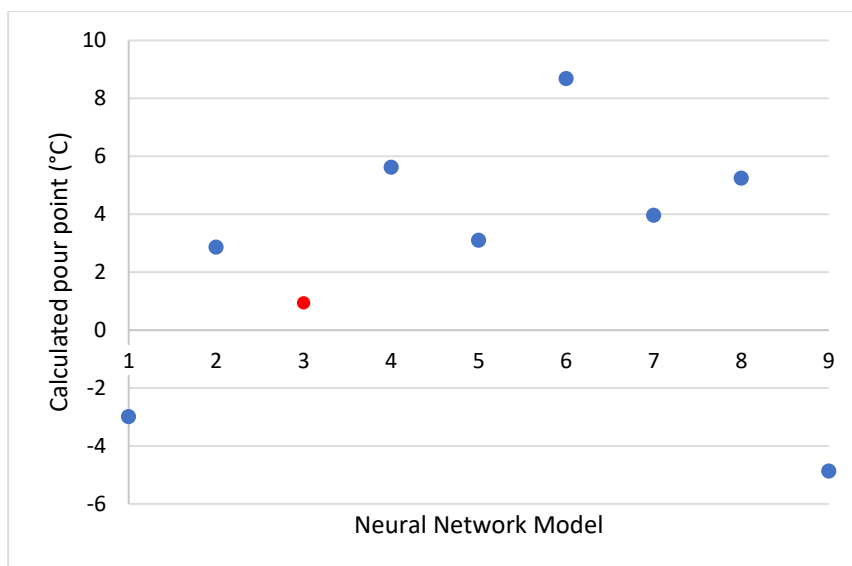


**Figure 23.** Validation of the modeled MLP-ANNs using the experimental dataset given in Table 1

The best prediction of the pour point is obtained as 0.94 °C using the mentioned neural network. As

Figure 23 indicates, with the seven parameters simultaneously implemented as the input

parameters, the ANN does not yield satisfactory pour point prediction.

Figure 24 shows the results of the pour point prediction using the RBF neural networks for the experimental dataset given in Table 1. As it can be seen from the figure, the RBF

neural networks demonstrate poor predictive performance, even using ten number of the neurons in the hidden layer. In this case, the pour point is calculated as -32.2 °C (Point 1 in Figure 24), indicating a high deviation from the experimental value.

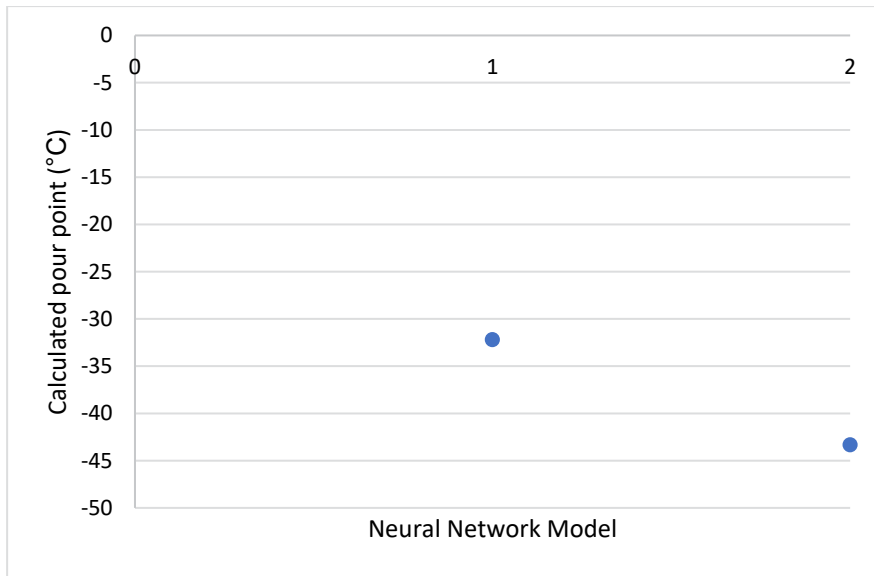


Figure 24. Validation of the modeled RBF-ANNs using the experimental dataset given in Table 1

With the five number of neurons implemented in the hidden layer (Point 2 in Figure 24), even worse pour point prediction is obtained. This type of the neural network changes the vector space of the data leading to the poor prediction of the pour point.

Comparing the mentioned neural networks, it can be concluded that the MLP-ANN is more precise than the RBF-ANN in predicting the pour point. Also, validation of these two types of the neural networks indicated that the MLP-ANN predicts the pour point more accurately than the RBF-ANN.

### 3.4. Non-linear equation for pour point prediction

In order to compare the predictive ability of the MLP-ANN with another model, a non-linear equation was developed, based on the data points given in Table A-1, to predict the pour point of crude oils as a function of wax content and cloud point, expressed by:

$$T_p = a + b \ln x_1 + c/x_2 + d \ln x_1^2 + e/x_2^2 + f (\ln x_1)/x_2 + g \ln x_1^3 + h/x_2^3 + i \ln x_1/x_2^2 + j \ln x_1^2/x_2 \quad (4)$$

Where  $T_p$  denotes the pour point in °C,  $x_1$  is the wax content in wt%, and  $x_2$  is the cloud point in °C. The values of the parameters  $a$  to  $j$  are given in Table 5.

Table 5. Parameters of Equation (4) for the pour point

Parameter	Value	Parameter	Value
$a$	-42.25	$f$	-1344.43
$b$	27.27	$g$	-2.99
$c$	2501.48	$h$	445349.02
$d$	13.094	$i$	16755.75
$e$	-68137.89	$j$	-45.68

Figure 25 shows the comparison between the experimental and the calculated pour point using Equation (4) and artificial neural network versus wax content and cloud point. The regression value obtained from the mathematical model is 62.87% and from the neural network model is 76.8%, representing the higher accuracy of the MLP neural network in predicting the pour point in comparison with the mathematical model. When applying the developed equation to the

experimental data set used in this study, the pour point of the crude oil sample was obtained as 6.22 °C, indicating a higher deviation from the measured value of 0 °C than that obtained using the MLP neural network (i.e., 0.94 °C).

### 3.5. Comparison of MLP neural network with empirical correlation

The capability of the developed artificial neural

network model in predicting the pour point was also compared with the generalized empirical correlation developed by Riazi and Daubert [42]. The correlation uses specific gravity, molecular weight and viscosity as the key input parameters, which is given in the following form:

$$T_p = 130.47[SG^{2.970566}] \times [MW^{(0.61235-0.47357SG)}] \times \left[ \frac{v_{38(100)}^{(0.310331-0.328345G)}}{38(100)} \right] \quad (5)$$

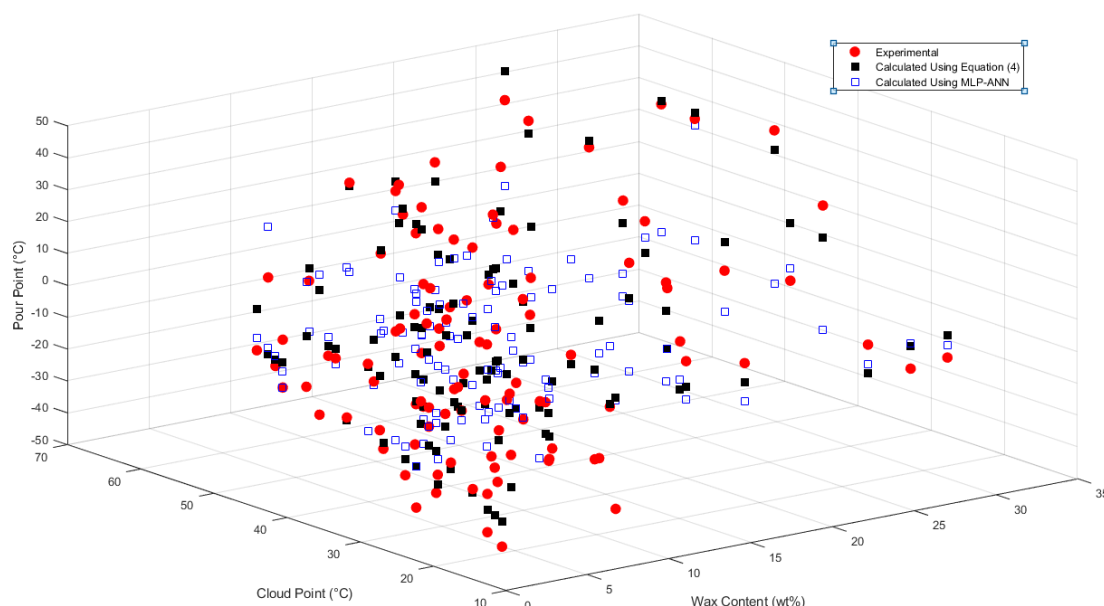


Figure 25. Comparison between experimental and calculated pour point using Equation (4) and artificial neural network versus wax content and cloud point

Where  $T_p$  is the pour point in kelvin, SG is specific gravity, MW is the molecular weight and  $U_{38(100)}$  denotes the kinematic viscosity at 37.8 °C (100 °F) in cSt.

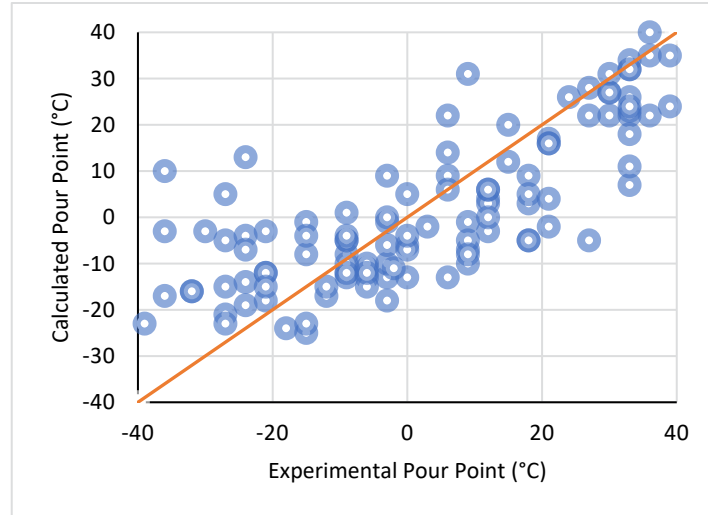
The parity plots of the calculated versus experimental values of the pour point using the artificial neural network model and the Riazi and Daubert's correlation are shown in Figures 26 (a) and (b), respectively. As it can be seen from the figures, the artificial neural network model predicts the pour points of the crude oil samples more accurately than the empirical correlation by Riazi and Daubert. According to Figure 26.b, the data points are highly scattered around the straight line passing through the origin with the slope of 1.0. The regression values of the MLP-ANN model and the empirical correlation are 76.8% and 0.24%,

respectively, confirming the higher accuracy of the MLP-ANN model in predicting the pour point than that obtained by applying the empirical correlation. The less accurate predictions from the empirical correlation may be attributed to the fact that the Riazi and Daubert's correlation was developed using the pour point data of the petroleum fractions. However, the constructed neural network model is based on the pour point data of crude oils. Furthermore, molecular weight and kinematic viscosity as the input parameters to the empirical equation are not available for all the crude oil samples used in this study. Consequently, their values were calculated using appropriate correlations given in Appendix B, which may affect the accuracy of pour point predictions.

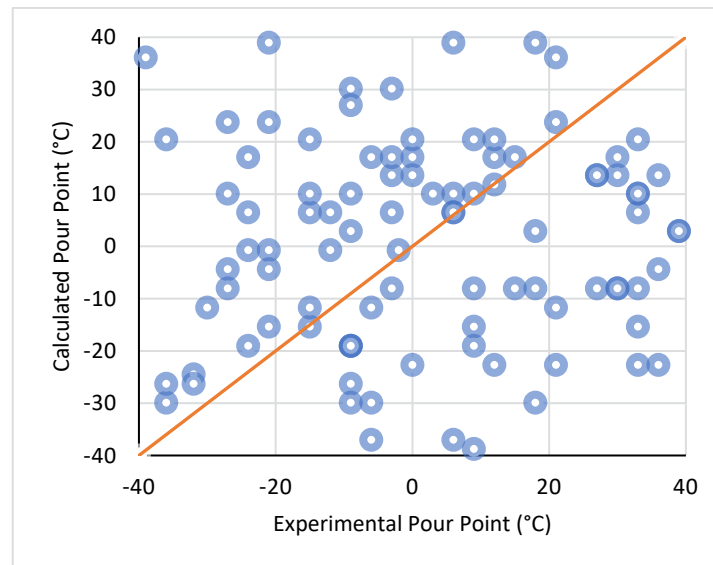
The details of the pour point calculations applying

the Riazi and Daubert's correlation, including the estimated pour points and the parameters used as

the input to the correlation are given in Table B-1.



(A)



(B)

**Figure 26.** Calculated versus experimental pour point of crude oil samples using (a) artificial neural network model, and (b) empirical equation by Riazi and Daubert

#### 4. Conclusion

For the first time, in this study the MLP and RBF artificial neural networks were constructed to predict the pour point of crude oils in a wide range of temperatures. The two networks were investigated in terms of their predictive accuracy.

Based on the results obtained in this study, the following conclusions can be derived:

- The modelled MLP-ANN indicated the best predictive performance when using the two parameters of cloud point and wax content as the input to the neural network. The regression

values of training, validation, and testing sets of this network were obtained as 79.5%, 74.1%, and 76.8%, respectively. Among the three activation functions used in this study, the Softmax-Softmax activation function was selected based on the predictive accuracy of the pour point.

- To evaluate the constructed MLP-ANN, it was implemented using an experimental dataset obtained for an oil sample. The absolute error of 0.94°C showed the high accuracy of the pour point prediction using this network.

- The experimental dataset was also used to validate the RBF-ANN. In this case, the pour point of the oil sample was obtained as -32.2 °C, indicating a high deviation from the measured value of 0°C. Consequently, the MLP-ANN is more effective than the RBF-ANN in terms of the predictive accuracy of the pour point.

- The comparison of the MLP-ANN with the developed mathematical equation in this study and the generalized empirical correlation by Riazi and Daubert confirmed the superiority of the modelled neural network in predicting the pour point over the empirical equations.

## References

- [1] O. Emmanuel, C. Wisdom, and O. Moses, "Determination of Cloud and Pour Point of Crude Oil with Reference to Crude Transportation."
- [2] T. J. Behbahani, A. A. M. Beigi, Z. Taheri, and B. Ghanbari, "Investigation of wax precipitation in crude oil: Experimental and modeling," *Petroleum*, vol. 1, no. 3, pp. 223-230, 2015.
- [3] A. S. Kasumu, "An Investigation of Solids Deposition from Two-Phase Wax-Solvent-Water Mixtures," doctoral thesis, University of Calgary, <http://dx.doi.org/10.11575/PRISM/24916>, 2014.
- [4] M. F. A. Zolkifli, "Crude Oil Pour Point Measurement By Using Rotational Method," Universiti Teknologi PETRONAS, URI: <http://utpedia.utp.edu.my/id/eprint/13887>, 2014.
- [5] Y. K. Anaya Jaimes, "Flow assurance of waxy crude oil= physical and chemical characterization, critical temperatures and rheological behavior for the restart problem-experimental study= Garantia de escoamento de óleos parafínicos: caracterização físico-química, temperaturas críticas e comportamento reológico em problemas de repartida-estudo experimental," 2016.
- [6] F. D. Santos *et al.*, "Improvement on pour point of heavy oils by adding organic solvents," *Revista Virtual de Química*, vol. 9, no. 6, 2017.
- [7] J. Taheri-Shakib, A. Shekarifard, and H. Naderi, "Characterization of the wax precipitation in Iranian crude oil based on Wax Appearance Temperature (WAT): Part 1. The influence of electromagnetic waves," *Journal of Petroleum Science and Engineering*, vol. 161, pp. 530-540, 2018.
- [8] A. Aiyejina, D. P. Chakrabarti, A. Pilgrim, and M. Sastry, "Wax formation in oil pipelines: A critical review," *International journal of multiphase flow*, vol. 37, no. 7, pp. 671-694, 2011.
- [9] M. Al-Marhoun, S. Ali, A. Abdulraheem, S. Nizamuddin, and A. Muhammadain, "Prediction of bubble point pressure from composition of black oils using artificial neural network," *Petroleum science and technology*, vol. 32, no. 14, pp. 1720-1728, 2014.
- [10] F. Alnaimat, M. Ziauddin, and B. Mathew, "Wax Deposition in Crude Oil Transport Lines and Wax Estimation Methods," in *Intelligent System and Computing*: IntechOpen, 2019.
- [11] A. Tatar, S. Naseri, N. Sirach, M. Lee, and A. Bahadori, "Prediction of reservoir brine properties using radial basis function (RBF) neural network," *Petroleum*, vol. 1, no. 4, pp. 349-357, 2015.
- [12] M. Narvekar and P. Fargose, "Daily weather forecasting using artificial neural network," *International Journal of computer applications*, vol. 121, no. 22, 2015.
- [13] Y. Wei, M. Wu, and L. Zhao, "Wax deposition rate model for crude oil pipeline based on neural network," in *2010 Sixth International Conference on Natural Computation*, 2010, vol. 2, pp. 760-762: IEEE.
- [14] M. I. Jahirul, R. J. Brown, W. Senadeera, I. M. O'Hara, and Z. D. Ristovski, "The use of artificial neural networks for identifying sustainable biodiesel feedstocks," *Energies*, vol. 6, no. 8, pp. 3764-3806, 2013.
- [15] C. Benamara, K. Gharbi, M. N. Amar, and B. Hamada, "Prediction of Wax Appearance Temperature Using Artificial Intelligent Techniques," *Arabian Journal for Science and Engineering*, vol. 45, no. 2, pp. 1319-1330, 2020.
- [16] P. Chidambaram, "Development and testing of an artificial neural network based history matching protocol to characterize reservoir properties," doctoral thesis, Department of Energy and Mineral Engineering, The Pennsylvania State University, 2009.
- [17] A. H. Fath, F. Madanifar, and M. Abbasi, "Implementation of multilayer perceptron (MLP) and radial basis function (RBF) neural networks to predict solution gas-oil ratio of crude oil systems," *Petroleum*, vol. 6, no. 1, pp. 80-91, 2020.
- [18] Y. Xie and Y. Xing, "A prediction method for the wax deposition rate based on a radial basis function neural network," *Petroleum*, vol. 3, no. 2, pp. 237-241, 2017.
- [19] A. S. Maheshwari and J. G. Chellani, "Correlations for Pour Point and Cloud Point of middle and heavy distillates using density and distillation temperatures," *Fuel*, vol. 98, pp. 55-60, 2012.
- [20] K. Hu *et al.*, "Application of bayesian regularized artificial neural networks to predict pour point of crude oil treated by pour point depressant," *Petroleum Science and Technology*, vol. 35, no. 13, pp. 1349-1354, 2017.
- [21] L. A. Alcazar-Vara and E. Buenrostro-Gonzalez, "Characterization of the wax precipitation in Mexican crude oils," *Fuel processing technology*, vol. 92, no. 12, pp. 2366-2374, 2011.
- [22] S. ALI, "SYNTHESIS, CHARACTERIZATION AND EVALUATION OF POUR POINT DEPRESSANTS FOR MALAYSIAN WAXY CRUDES," Universiti Teknologi PETRONAS, 2013.
- [23] S. Allenson and A. Johnston, "Comparison of different experimental techniques used for wax deposition testing,"

- 2008.
- [24] R. Bansal, R. Burla, K. Afzal, and S. S. Sharma, "Dynamic simulation for Optimizing Pigging Frequency for Dewaxing," in *SPE Oil and Gas India Conference and Exhibition*, 2012: Society of Petroleum Engineers.
- [25] R. Capitello and L. Sirieix, "Consumers' perceptions of sustainable wine: an exploratory study in France and Italy," *Economies*, vol. 7, no. 2, p. 33, 2019.
- [26] L. V. Castro and F. Vazquez, "Fractionation and characterization of Mexican crude oils," *Energy & fuels*, vol. 23, no. 3, pp. 1603-1609, 2009.
- [27] A. Gupta and A. Sircar, "Wax deposition modelling and comparison with field data for some Indian oil fields," *STM. J.*, vol. 4, pp. 1-15, 2017.
- [28] A. Japper-Jaafar, P. Bhaskoro, and Z. Mior, "A new perspective on the measurements of wax appearance temperature: Comparison between DSC, thermomicroscopy and rheometry and the cooling rate effects," *Journal of petroleum science and Engineering*, vol. 147, pp. 672-681, 2016.
- [29] P. Jokuty, M. Fingas, E. Meyer, C. Knobel, and S. Whitar, "Hydrocarbon groups and their relationships to oil properties and behaviour," in *ARCTIC AND MARINE OILSPILL PROGRAM TECHNICAL SEMINAR*, 1995, pp. 1-20: MINISTRY OF SUPPLY AND SERVICES, CANADA.
- [30] M. C. Khalil De Oliveira and M. A. Gonçalves, "An effort to establish correlations between Brazilian crude oils properties and flow assurance related issues," *Energy & fuels*, vol. 26, no. 9, pp. 5689-5701, 2012.
- [31] S. Kumar and V. Mahto, "Emulsification of Indian heavy crude oil in water for its efficient transportation through offshore pipelines," *Chemical Engineering Research and Design*, vol. 115, pp. 34-43, 2016.
- [32] N. Makwashi, K. Sarkodie, S. Akubo, D. Zhao, and P. Diaz, "Investigation of the Severity of Wax Deposition in Bend Pipes Under Subcooled Pipelines Conditions," in *SPE Europec featured at 81st EAGE Conference and Exhibition*, 2019: Society of Petroleum Engineers.
- [33] H. M. Meighani, C. Ghotbi, T. J. Behbahani, and K. Sharifi, "A new investigation of wax precipitation in Iranian crude oils: Experimental method based on FTIR spectroscopy and theoretical predictions using PC-SAFT model," *Journal of Molecular Liquids*, vol. 249, pp. 970-979, 2018.
- [34] P. L. Perez *et al.*, "Mitigating wax deposition from crude oils: Correlations between physical-chemical properties of crude oils and the performance of wax inhibitors," in *Offshore Technology Conference*, 2016: Offshore Technology Conference.
- [35] R. Sharma, V. Mahto, and H. Vuthaluru, "Synthesis of PMMA/modified graphene oxide nanocomposite pour point depressant and its effect on the flow properties of Indian waxy crude oil," *Fuel*, vol. 235, pp. 1245-1259, 2019.
- [36] H. P. Soni, K. Agrawal, A. Nagar, and D. Bharambe, "Designing maleic anhydride- $\alpha$ -olefin copolymeric combs as wax crystal growth nucleators," *Fuel Processing Technology*, vol. 91, no. 9, pp. 997-1004, 2010.
- [37] P. Swivedi, C. Sarica, and W. Shang, "Experimental study on wax-deposition characteristics of a waxy crude oil under single-phase turbulent-flow conditions," *Oil and Gas Facilities*, vol. 2, no. 04, pp. 61-73, 2013.
- [38] M. Theyab and P. Diaz, "Experimental Study on the Effect of Polyacrylate Polymer (C16-C22) on Wax Deposition," in *7th International Conference on Chemical Engineering and Applications (CCEA 2016)*, 2016: London South Bank University.
- [39] M. Theyab and P. Diaz, "Experimental study of wax deposition in pipeline—effect of inhibitor and spiral flow," *International Journal of Smart Grid and Clean Energy*, vol. 5, no. 3, pp. 174-181, 2016.
- [40] L. C. Vieira, M. B. Buchuid, and E. F. Lucas, "Effect of pressure on the crystallization of crude oil waxes. II. Evaluation of crude oils and condensate," *Energy & Fuels*, vol. 24, no. 4, pp. 2213-2220, 2010.
- [41] B. Yao *et al.*, "Organically modified nano-clay facilitates pour point depressing activity of polyoctadecylacrylate," *Fuel*, vol. 166, pp. 96-105, 2016.
- [42] M. Riazi, *Characterization and properties of petroleum fractions*. ASTM international, 2005.
- [43] T. Ahmed, *Reservoir engineering handbook*. Gulf professional publishing, 2018.
- [44] D. K. Gold, W. D. McCain, Jr., and J. W. Jennings, "An Improved Method for the Determination of the Reservoir-Gas Specific Gravity for Retrograde Gases (includes associated papers 20006 and 20010 )," *Journal of Petroleum Technology*, vol. 41, no. 07, pp. 747-752, 1989.

Appendix A

Table A-1. Data points used to train, validate and test the neural networks

Number of data set	Pour point (°C)	°API	Wax Content (wt%)	Saturate (wt%)	Aromatic (wt%)	Resin (wt%)	Asphaltene (wt%)	Cloud point (°C)
1	27	35	19.7	73.25	21.2	5.14	0.41	35
2	-24	33	1.2	57.4	30.8	10.4	1.4	22
3	-30	36	11.26	41.7	34.2	21.8	2.3	23
4	-24	28	10.91	41.8	28.7	28.4	1.5	32
5	0	38	15.06	46.81	37.13	15.63	0.01	19
6	-9	41	10.17	44.03	38.32	16.65	0.01	18.5
7	-36	33	13.77	42.72	38.47	17.86	0.31	28
8	-21	30	3.02	38.44	14.59	41.44	5.53	34
9	-24	21	3.83	26.53	14.74	47.6	11.13	31
10	-12	16	4.27	10.49	9	64.12	16.39	20.5
11	24	27	10.6	51.2	24.2	23.1	1.5	46
12	6	27	10	54.5	23	22	0.5	40
13	12	28	5.6	57.1	24.5	18	0.4	35
14	6	28	7.1	53.8	22	23.7	0.5	35
15	9	28	15.4	56.2	25.7	17.1	1	41
16	6	29	24.8	54	24	22	0.5	35.5
17	6	29	5.6	57.7	24.2	17.4	0.7	37
18	-27	29	6.5	52.7	33.6	12.6	1.1	26.5
19	0	29.5	5.8	56.6	24.4	19	0.5	34.5
20	-36	30	7.1	51.1	30.9	16.6	1.4	27
21	15	31	10.8	57.2	26.2	14.7	2	36.5
22	30	35	20.15	74.91	20.44	4.26	0.39	39
23	12	31	6.21	52.2	41.57	1.97	3.02	32
24	0	37	5.02	56.26	36.61	1.97	3.21	27
25	30	31	9.73	56.38	28.96	4.73	8.74	41
26	27	30	11.15	57.36	26.69	5.05	8.91	49
27	12	36	9.98	67.6	24.05	3.92	2.04	29
28	3	36	10.25	62.35	27.9	3.14	3.04	24
29	-15	39	4	91.5	6.7	0.5	1.3	13
30	-9	27	3	61.2	23.5	9.3	6	29
31	33	40	7.8	70.7	29.3	0	5	32
32	33	41	8	98.2	0.9	0.45	1.17	35
33	33	39	11.5	92.4	6	0.45	0.45	37
34	33	27	10.5	62.7	24.1	8.2	0	45
35	-3	43.5	5.6	90.6	6.9	1.1	1.4	22
36	9	45	13.8	92.2	6.6	0.1	1.1	17
37	21	39.5	8.2	89	8.1	1.3	1.6	26
38	42	34	14.9	82.4	15.5	0.8	1.3	44
39	21	34	30.6	89.9	8	0.8	1.3	35
40	33	33	33	89.9	8	0.8	1.3	47
41	27	22	3.9	89.9	8	0.8	1.3	30
42	-9	30	3	54	32	7	6	28
43	-3	24	3	42	44	7	7	40
44	-3	21	3	40	46	8	7	41
45	9	17	4	27	54	9	10	34
46	-6	38	5	72	23	4	1	24
47	-9	13	4	15	50	16	19	37
48	0	37	6	81	16	3	1	22
49	9	35	6	78	17	4	1	26
50	9	33	6	77	15	7	1	27
51	12	32	7	78	16	5	1	27
52	-6	12	7	25	73	2	0	21
53	-36	27	1	51	39	9	1	24.5
54	-27	24	1	46	43	10	1	26
55	-21	22	1	44	44	11	1	29
56	-15	20	1	42	43	14	1	34
57	-32	31	2	59	35	5	1	24
58	-32	28	2	58	35	6	1	24
59	-15	20	3	32	38	14	16	44
60	-27	35	2	73	21	4	1	19
61	-21	31	2	69	25	5	0	22

Number of data set	Pour point (°C)	°API	Wax Content (wt%)	Saturate (wt%)	Aromatic (wt%)	Resin (wt%)	Asphaltene (wt%)	Cloud point (°C)
62	-12	29	2	66	27	6	0	25
63	-6	26	2	64	29	7	0	25
64	-15	21	2	38	39	8	16	45
65	-9	17	2	33	41	8	18	46
66	0	15	2	31	41	10	17	45
67	18	12	2	28	39	11	22	47
68	-39	35	2	71	25	4	0	17
69	-9	35	3	57	34	7	2	25
70	-9	34	7	71	21	5	4	25.5
71	18	30	7	68	24	5	3	31
72	18	27	7	65	24	6	4	36
73	21	25	8	61	27	6	6	45
74	-42	39	2	79	15	6	0	15
75	-9	36	4	71	20	8	1	25
76	-3	31	4	67	26	7	1	26
77	9	29	4	64	27	8	1	28
78	12	26	5	61	28	9	2	32
79	-27	35	2	78	16	5	0	17
80	-2	38	4	68	26	5	1	25.5
81	18	20	2	46	30	13	10	47
82	39	31	10	72	13	8	6	47
83	-18	45	2	81	18	1	0	16
84	-15	43	3	87	10	3	0	16
85	-3	39	6	85	14	2	0	18
86	21	31	16.5	69.3	22.2	7.5	1	30
87	33	38	31.26	84.97	12.99	1.01	0.54	54
88	-42	41	10.75	65.77	24.65	8.56	1.02	19
89	-24	39	8.653	63.56	26.99	7.55	1.9	23
90	33	29	11.42	48.93	40.06	7.77	3.24	34.5
91	39	28	14	66	12	15.5	1.5	51
92	30	35	20.15	74.91	20.44	4.26	0.39	39
93	-24	35	7.1	73.1	15.6	8.3	3	20
94	-3	32	29.5	50.81	37.57	10.84	0.79	37
95	-21	43	30.6	58.33	36.18	4.47	1	23
96	-21	40	33.3	55.38	33.61	10.64	0.37	24
97	-3	30	18.2	49.26	42.4	8.14	0.2	18
98	-6	37	26.2	66.01	28.54	5.35	0.1	19
99	33	37	23.89	76.23	2.89	20.75	0.13	52
100	15	40	17.86	76.73	17.73	5.74	0.2	28
101	18	36	16.15	64.3	26.94	8.7	0.06	24
102	6	28	0.28	51.8	21.9	25.6	0.75	29.5
103	36	30	30.55	80.78	10.22	8.02	0.98	57
104	33	38	31.26	84.97	12.99	1.5	0.54	54
105	12	44	5.4	72.9	17	9.7	0.4	49
106	-9	41	3.1	79.6	14	6.2	0.2	51
107	36	48	25	61.4	17.5	18.7	2.3	66
108	-27	20	4.7	45.2	26.2	25.6	3.1	46
109	-6	45	2.4	86	13.8	0	0	27
110	42	32	21.3	71.8	19.9	9.3	1.4	54.5
111	36	32	11.29	63.19	28.1	8.61	0.1	37
112	21	31	16.5	69.3	22.2	7.5	1	30
113	33	26	10.56	70.87	24.04	4.77	0.32	55
114	30	30	12.49	66.89	26.94	5.88	0.29	53

### Appendix B

According to Table A-1, among the three input parameters of Equation (5), only API gravity and hence, specific gravity is available in the data sets used to calculate the pour point. The other two parameters are not given for all the data. Therefore, their values were estimated using appropriate correlations. To do so, the viscosities

of the crude oils used in this study were estimated using the Beal's correlation. This correlation was first developed graphically by Beal (1946) using a total of 753 values for deal-oil viscosity at and above 100 °F. Then, it was expressed in the following mathematical relationship by Standing (1981)[43]:

$$\mu_o = (0.32 + \frac{1.8(10^7)}{API^{4.53}}) (\frac{360}{T - 260})^a \tag{B-1}$$

$$a = 10^{(0.43 + 8.33/API)} \tag{B-2}$$

Where  $\mu_o$  is the deal oil viscosity in cp, as measured at 14.7 psia and specified temperature, and  $T$  is the temperature in °R.

In order to calculate the kinematic viscosity, the density of crude oil is required in addition to the viscosity. The density of crude oil was estimated using the following correlation based on SG as the input parameter[42]:

$$\rho_o = 0.999 SG - 10^{-3} \times (2.34 - 1.898 SG) \times (T - 288.7) \tag{B-3}$$

Where SG is the specific gravity at 15.5 °C (60 °F/60 °F) and  $T$  is the absolute temperature in K.  $\rho_o$  is the oil density in g/cm<sup>3</sup> at temperature and atmospheric pressure. The kinematic viscosity at the desired temperature was then calculated as the following:

$$v_o = \mu_o / \rho_o \tag{B-4}$$

For the data sets where the molecular weight is not available, the molecular weight of the crude oil was estimated using the following correlation[44]:

$$MW = \frac{5954}{\text{°API} - 8.8} = \frac{42.43SG}{1.008 - SG} \tag{B-5}$$

**Table B-1.** Input parameter values and calculated pour points using Riazi and Daubert’s empirical correlation

°API	SG	MW	Density(gr/cm <sup>3</sup> )	Viscosity(cp)	Kinematic viscosity(cSt)	Calculated Pour point (K)	Calculated Pour point (°C)	Experimental pour point (°C)
35	0.850	227.3	0.833	4.598	5.521	265	-8	27
33	0.860	246.0	0.844	6.068	7.193	272	-1	-24
36	0.845	218.9	0.828	4.037	4.879	261	-12	-30
28	0.887	310.1	0.872	13.645	15.654	290	17	0
38	0.835	203.9	0.817	3.163	3.871	254	-19	-9
41	0.820	184.9	0.802	2.276	2.838	243	-30	-36
33	0.860	246.0	0.844	6.068	7.193	272	-1	-21
30	0.876	280.8	0.860	9.652	11.220	283	10	6
21	0.928	488.0	0.914	63.369	69.326	312	39	6
16	0.959	826.9	0.947	324.718	342.960	325	51	-27
27	0.893	327.1	0.877	16.432	18.726	294	20	0
27	0.893	327.1	0.877	16.432	18.726	294	20	-36
28	0.887	310.1	0.872	13.645	15.654	290	17	15
28	0.887	310.1	0.872	13.645	15.654	290	17	30
28	0.887	310.1	0.872	13.645	15.654	290	17	12
29	0.882	294.8	0.866	11.430	13.200	287	14	0
29	0.882	294.8	0.866	11.430	13.200	287	14	30
29	0.882	294.8	0.866	11.430	13.200	287	14	27
29.5	0.879	287.6	0.863	10.493	12.158	285	12	12
30	0.876	280.8	0.860	9.652	11.220	283	10	3
31	0.871	268.2	0.855	8.212	9.609	280	7	-15
35	0.850	227.3	0.833	4.598	5.521	265	-8	33
31	0.871	268.2	0.855	8.212	9.609	280	7	33
37	0.840	211.1	0.822	3.564	4.334	258	-15	33
31	0.871	268.2	0.855	8.212	9.609	280	7	-3
30	0.876	280.8	0.860	9.652	11.220	283	10	9
36	0.845	218.9	0.828	4.037	4.879	261	-12	21
36	0.845	218.9	0.828	4.037	4.879	261	-12	42
39	0.830	197.2	0.812	2.821	3.474	250	-23	21
27	0.893	327.1	0.877	16.432	18.726	294	20	33
40	0.825	190.8	0.807	2.528	3.133	247	-26	-9
41	0.820	184.9	0.802	2.276	2.838	243	-30	-6
39	0.830	197.2	0.812	2.821	3.474	250	-23	0
27	0.893	327.1	0.877	16.432	18.726	294	20	9
43.5	0.809	171.6	0.790	1.785	2.260	234	-39	9
45	0.802	164.5	0.783	1.563	1.996	229	-44	12
39.5	0.827	193.9	0.810	2.669	3.297	249	-24	-32
34	0.855	236.3	0.838	5.267	6.283	269	-4	-27
34	0.855	236.3	0.838	5.267	6.283	269	-4	-21
33	0.860	246.0	0.844	6.068	7.193	272	-1	-12
22	0.922	451.1	0.908	48.898	53.866	309	36	-39
30	0.876	280.8	0.860	9.652	11.220	283	10	-9

°API	SG	MW	Density(gr/cm <sup>3</sup> )	Viscosity(cp)	Kinematic viscosity(cSt)	Calculated Pour point (K)	Calculated Pour point (°C)	Experimental pour point (°C)
24	0.910	391.7	0.895	30.474	34.034	303	30	-9
21	0.928	488.0	0.914	63.369	69.326	312	39	18
17	0.953	726.1	0.940	220.833	234.907	322	49	-42
38	0.835	203.9	0.817	3.163	3.871	254	-19	-9
13	0.979	1417.6	0.968	1399.909	1446.862	332	59	-3
37	0.840	211.1	0.822	3.564	4.334	258	-15	9
35	0.850	227.3	0.833	4.598	5.521	265	-8	-27
33	0.860	246.0	0.844	6.068	7.193	272	-1	-2
32	0.865	256.6	0.849	7.036	8.286	276	3	39
12	0.986	1860.6	0.975	2667.464	2736.833	336	63	-18
27	0.893	327.1	0.877	16.432	18.726	294	20	-15
24	0.910	391.7	0.895	30.474	34.034	303	30	-3
22	0.922	451.1	0.908	48.898	53.866	309	36	21
20	0.934	531.6	0.920	83.615	90.842	315	42	33
31	0.871	268.2	0.855	8.212	9.609	280	7	-42
28	0.887	310.1	0.872	13.645	15.654	290	17	-24
20	0.934	531.6	0.920	83.615	90.842	315	42	33
35	0.850	227.3	0.833	4.598	5.521	265	-8	30
31	0.871	268.2	0.855	8.212	9.609	280	7	-24
29	0.882	294.8	0.866	11.430	13.200	287	14	-3
26	0.898	346.2	0.883	19.975	22.612	297	24	-21
21	0.928	488.0	0.914	63.369	69.326	312	39	-21
17	0.953	726.1	0.940	220.833	234.907	322	49	-3
15	0.966	960.3	0.954	498.239	522.466	327	54	-6
12	0.986	1860.6	0.975	2667.464	2736.833	336	63	33
35	0.850	227.3	0.833	4.598	5.521	265	-8	15
35	0.850	227.3	0.833	4.598	5.521	265	-8	18
34	0.855	236.3	0.838	5.267	6.283	269	-4	36
30	0.876	280.8	0.860	9.652	11.220	283	10	33
27	0.893	327.1	0.877	16.432	18.726	294	20	12
25	0.904	367.5	0.889	24.533	27.585	300	27	-9
39	0.830	197.2	0.812	2.821	3.474	250	-23	36
36	0.845	218.9	0.828	4.037	4.879	261	-12	-6
31	0.871	268.2	0.855	8.212	9.609	280	7	42
29	0.882	294.8	0.866	11.430	13.200	287	14	36
26	0.898	346.2	0.883	19.975	22.612	297	24	21
35	0.850	227.3	0.833	4.598	5.521	265	-8	30
38	0.835	203.9	0.817	3.163	3.871	254	-19	-24
20	0.934	531.6	0.920	83.615	90.842	315	42	-24
31	0.871	268.2	0.855	8.212	9.609	280	7	-12
45	0.802	164.5	0.783	1.563	1.996	229	-44	24
43	0.811	174.1	0.792	1.870	2.360	236	-37	6
39	0.830	197.2	0.812	2.821	3.474	250	-23	12
31	0.871	268.2	0.855	8.212	9.609	280	7	6
38	0.835	203.9	0.817	3.163	3.871	254	-19	9
41	0.820	184.9	0.802	2.276	2.838	243	-30	-9
39	0.830	197.2	0.812	2.821	3.474	250	-23	33
29	0.882	294.8	0.866	11.430	13.200	287	14	27
28	0.887	310.1	0.872	13.645	15.654	290	17	-3
35	0.850	227.3	0.833	4.598	5.521	265	-8	-3
35	0.850	227.3	0.833	4.598	5.521	265	-8	9
32	0.865	256.6	0.849	7.036	8.286	276	3	-9
43	0.811	174.1	0.792	1.870	2.360	236	-37	-6
40	0.825	190.8	0.807	2.528	3.133	247	-26	-36
30	0.876	280.8	0.860	9.652	11.220	283	10	-27
37	0.840	211.1	0.822	3.564	4.334	258	-15	-21
37	0.840	211.1	0.822	3.564	4.334	258	-15	-15
40	0.825	190.8	0.807	2.528	3.133	247	-26	-32
36	0.845	218.9	0.828	4.037	4.879	261	-12	-15
28	0.887	310.1	0.872	13.645	15.654	290	17	-6
30	0.876	280.8	0.860	9.652	11.220	283	10	-15
38	0.835	203.9	0.817	3.163	3.871	254	-19	-9
44	0.806	169.1	0.787	1.706	2.166	233	-41	0
41	0.820	184.9	0.802	2.276	2.838	243	-30	18
48	0.788	151.9	0.769	1.229	1.599	219	-54	18
20	0.934	531.6	0.920	83.615	90.842	315	42	21

°API	SG	MW	Density(gr/cm <sup>3</sup> )	Viscosity(cp)	Kinematic viscosity(cSt)	Calculated Pour point (K)	Calculated Pour point (°C)	Experimental pour point (°C)
45	0.802	164.5	0.783	1.563	1.996	229	-44	12
32	0.865	256.6	0.849	7.036	8.286	276	3	18
32	0.865	256.6	0.849	7.036	8.286	276	3	39
31	0.871	268.2	0.855	8.212	9.609	280	7	6
26	0.898	346.2	0.883	19.975	22.612	297	24	-27
30	0.876	280.8	0.860	9.652	11.220	283	10	33

## مطالعه آزمایشگاهی و پیش‌بینی دمای نقطه ریزش با استفاده از هوش مصنوعی

مریم محمودی کوهی<sup>۱</sup>، الناز خداپناه<sup>۲\*</sup>

۱. کارشناس ارشد مهندسی نفت، دانشکده مهندسی نفت و گاز، دانشگاه صنعتی سهند تبریز، تبریز، ایران
۲. دانشیار مهندسی نفت، دانشکده مهندسی نفت و گاز، دانشگاه صنعتی سهند تبریز، شهر جدید سهند، تبریز، ایران

### چکیده

نقطه ریزش به عنوان یک ویژگی فیزیکی مهم نفت خام، معیار سیالیت در دمای پایین است. تعیین دقیق این ویژگی از اهمیت زیادی برخوردار است؛ زیرا کاهش دما زیر نقطه ریزش نفت خام باعث مشکلات شدید تولید و حمل و نقل می‌شود. در این مطالعه، برای اولین بار، دو نوع شبکه عصبی مصنوعی (ANN)، شامل پرسپترون چند لایه (MLP) و شبکه عصبی پایه شعاعی (RBF)، برای پیش‌بینی نقطه ریزش پیشنهاد شده است. ابتدا، شبکه MLP با استفاده از روش‌های مختلف مدل‌سازی و ارزیابی شده است. بدین منظور، تعداد بهینه پارامترهای ورودی و بهترین تابع فعال‌سازی مورد بررسی قرار گرفته است. نتایج نشان می‌دهد که بهترین مدل پیش‌بینی کننده شبکه عصبی MLP با استفاده از دو پارامتر مقدار واکس و نقطه ابری شدن و تابع فعال‌سازی SoftMax-SoftMax ساخته می‌شود. رگرسیون مجموعه داده‌های آموزش، اعتبارسنجی و تست شبکه MLP مدل شده به ترتیب ۷۹/۵، ۷۴/۱ و ۷۶/۸ درصد است. برای اعتبارسنجی MLP-ANN ساخته شده، تعدادی آزمایش روی یک نمونه نفت خام انجام شده است. سپس، مجموعه داده به دست آمده از آزمایش‌ها برای پیش‌بینی نقطه ریزش استفاده می‌شود. خطای مطلق ۰/۹۴ درصد سانتیگراد نشان دهنده عملکرد عالی MLP-ANN در پیش‌بینی نقطه ریزش است. در نهایت، عملکرد پیش‌بینی MLP-ANN با RBF-ANN مقایسه می‌شود. نتایج دقت پیش‌بینی بالاتر MLP-ANN را در مقایسه با RBF-ANN نشان می‌دهد. بر اساس نتایج به دست آمده، MLP-ANN پیشنهادی را می‌توان با اطمینان به جای اندازه‌گیری‌های آزمایشگاهی گران و زمان‌بر برای تعیین نقطه ریزش نفت خام استفاده کرد.

### مشخصات مقاله

تاریخچه مقاله:

دریافت: ۲۳ دی ۱۳۹۹

دریافت پس از اصلاح: ۲۱ شهریور ۱۴۰۰

پذیرش نهایی: ۲۲ شهریور ۱۴۰۰

کلمات کلیدی:

نقطه ریزش

شبکه عصبی پرسپترون چند لایه

شبکه عصبی پایه شعاعی

مقدار واکس

نقطه ابری شدن

\*عهدنامه مکاتبات: الناز خداپناه

رایانامه: khodapanah@sut.ac.ir

تلفن: ۴۱۳۳۴۵۹۴۸۲

نحوه استناد به این مقاله:

Mahmoudi Kouhi M, Khodapanah E. Experimental Investigation and Prediction of Pour Point Using Artificial Intelligence, Journal of Oil, Gas and Petrochemical Technology, 2022; 9(1): 49-74. DOI:10.22034/jogpt.2023.268812.1085.